Diffraction results from ALICE

Diffraction and Low-x 2024

8-14 September 2024

Palermo, Sicily

Ernesto Calvo Villar
on behalf of the ALICE Collaboration
Pontificia Universidad Católica del Perú

Hadronic cross sections

- Energy dependence of the hadronic cross sections is hard to understand within QCD.
- Within the framework of Regge theory they are described by the exchange of trajectories.
- These trajectories can be approximated as linear functions of *t* (|t|=m²) at low t values.

$$\alpha(t) = \alpha(0) + \alpha' t \text{ (Mandelstam-t)}$$

- And their contribution to the total cross section is:

$$\sigma_{s\to\infty} \sim \frac{1}{s}\mathrm{Im}A(s,t=0)_{s\to\infty} \sim s^{\alpha(0)-1}$$

- All known meson trajectories have intercepts that are smaller than unity. This leads to the prediction that the total cross section for hadron scattering decreases with energy.

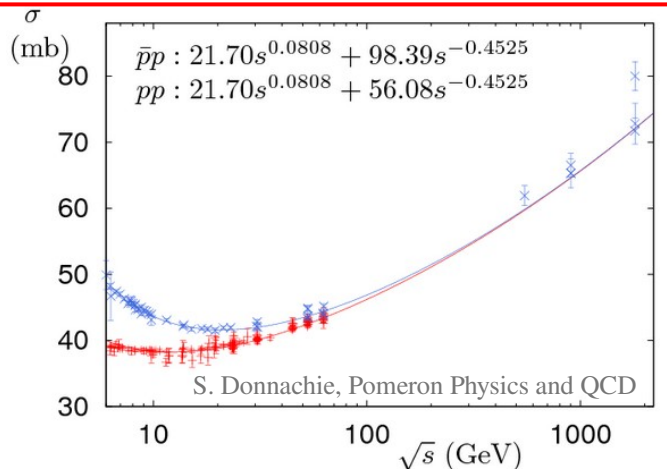

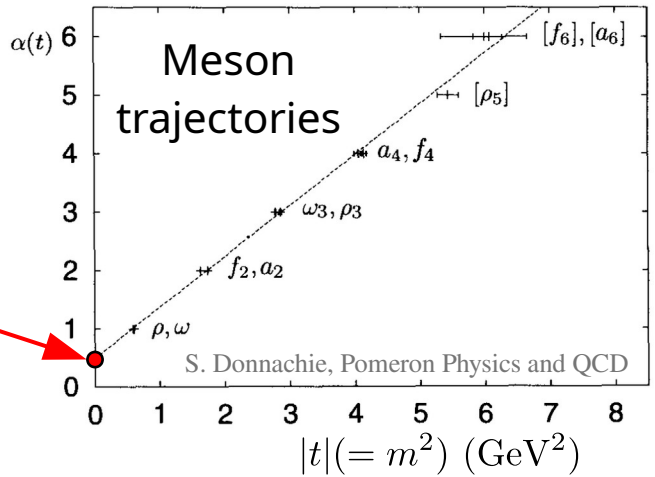

The pomeron trajectory

- Contribution of Regge trajectories to the total cross section is:

$$\sigma_{s\to\infty} \sim \frac{1}{s}\mathrm{Im}A(s,t=0)_{s\to\infty} \sim s^{\alpha(0)-1}$$

- The explanation for rising hadronic cross sections in terms of Regge theory is a new trajectory with intercept greater than unity.
- This trajectory was named the **pomeron** after the Ukrainian Soviet physicist Isaak Pomeranchuk.

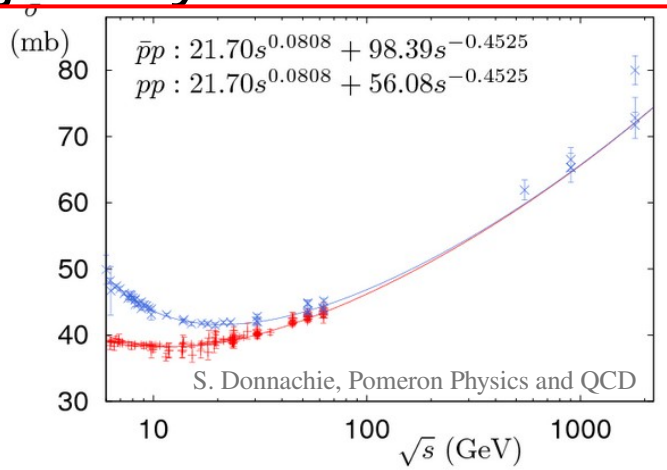

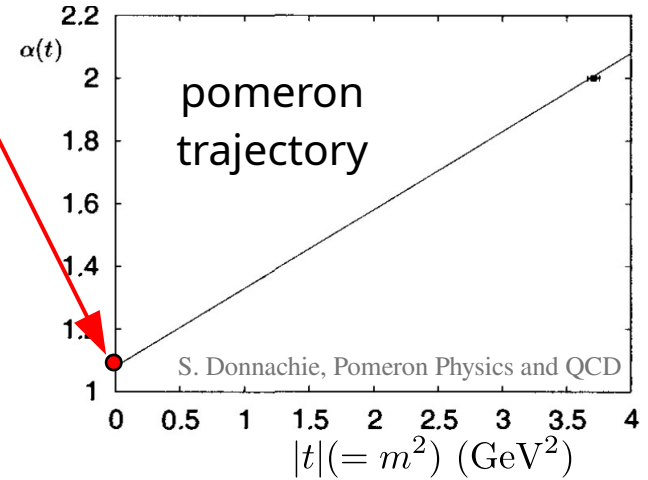

Inelastic and diffractive events

$$\sigma_{inel} = \sigma_{SD} + \sigma_{DD} + \sigma_{CD} + \sigma_{Non\text{-}Diff}$$

- Diffractive events, exchange of pomerons

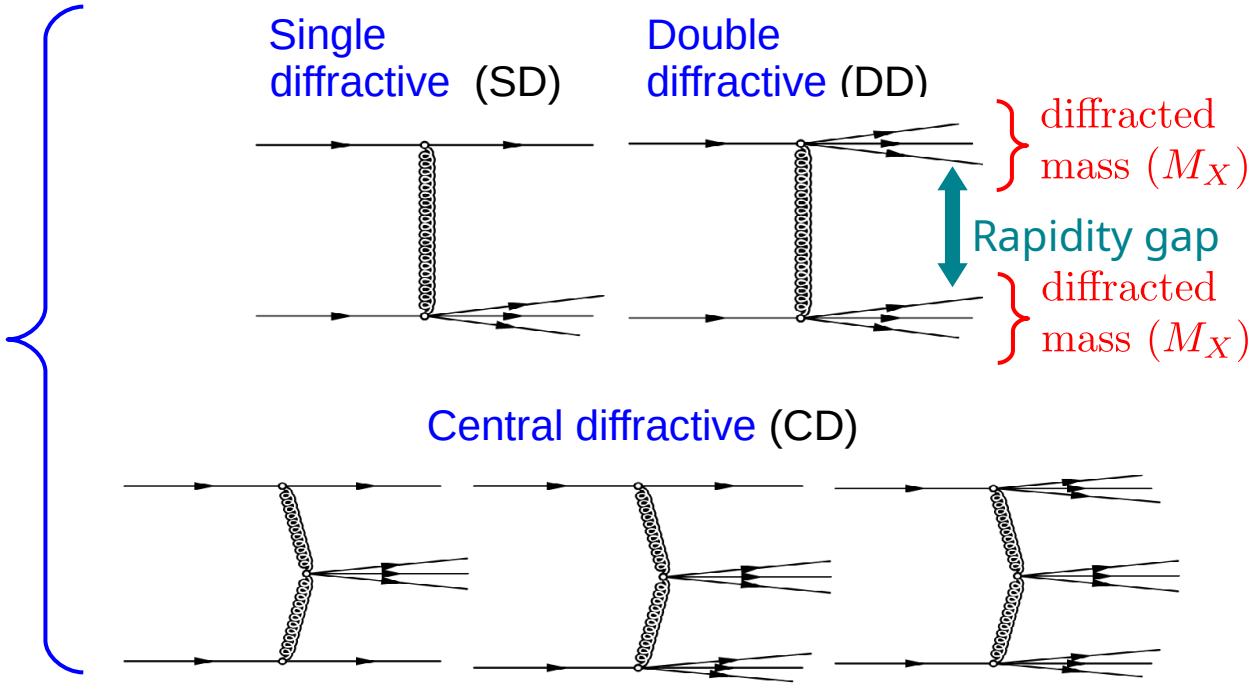

- Non-diffractive events (ND).
  No gap, no pomeron exchange

Diffraction in Run I

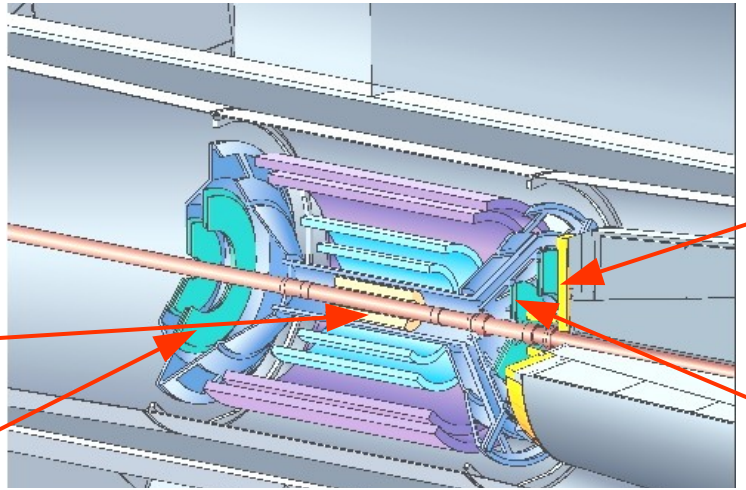

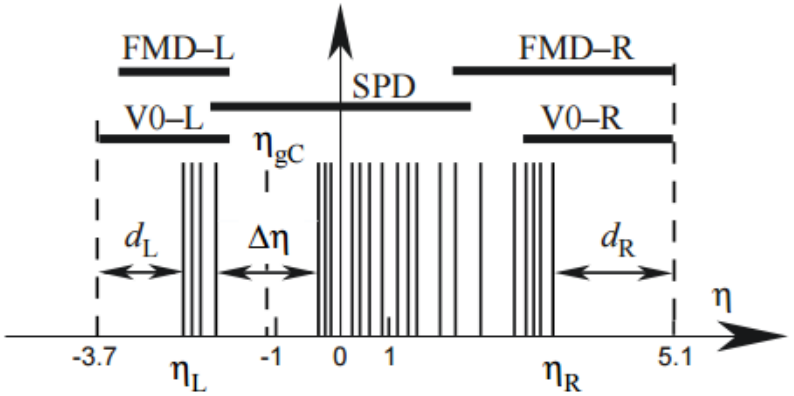

Diffraction in Run I: MC adjustment

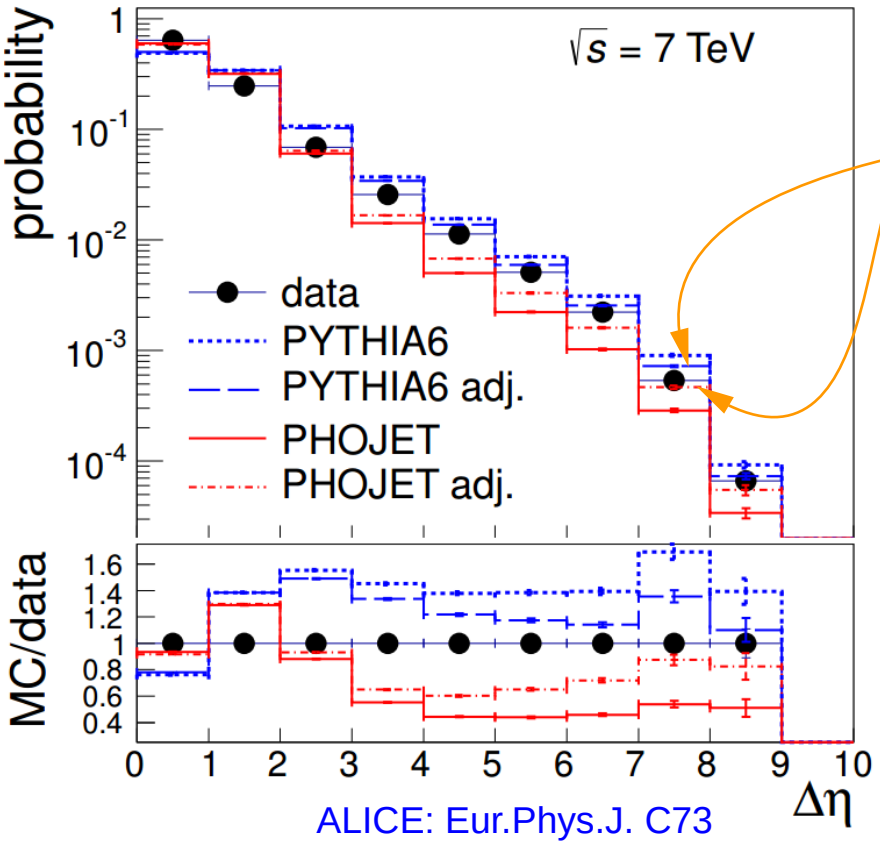

Adjusted DD content

ALICE: Eur.Phys.J. C73 (2013) no.6, 2456

Diffraction in Run I: Results

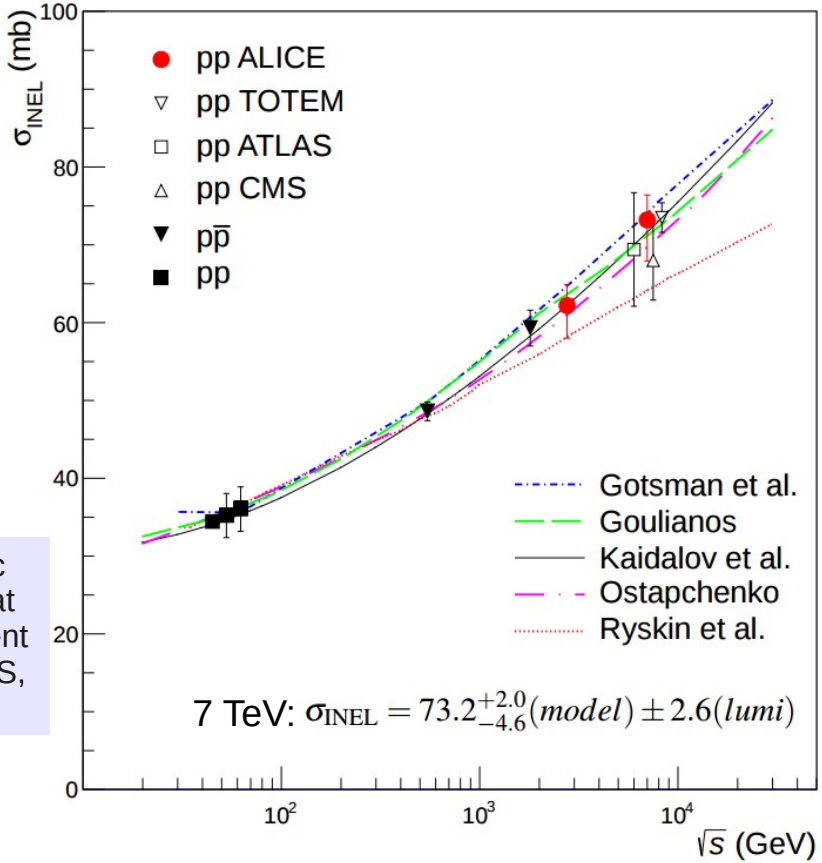

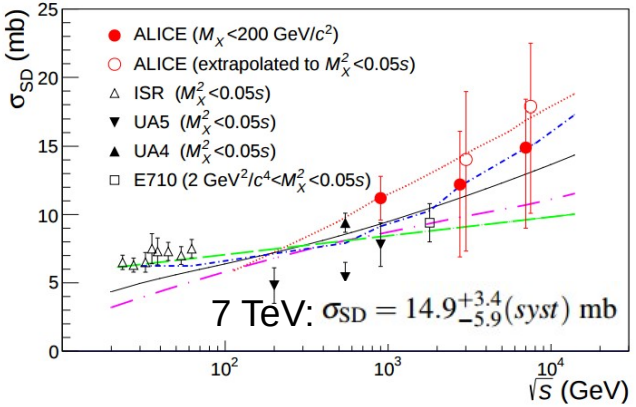

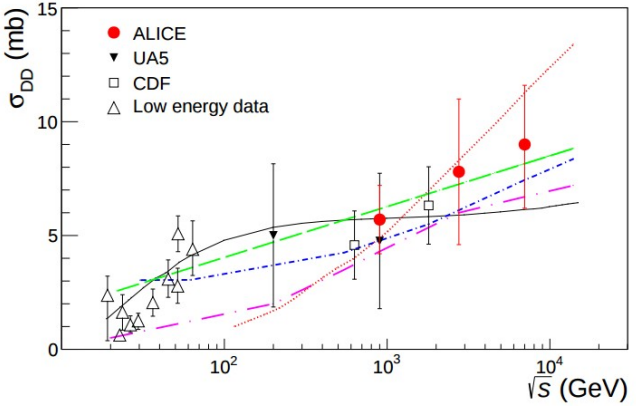

"The ALICE inelastic cross section result at √s = 7 TeV is consistent with those from ATLAS, CMS, and TOTEM"

ALICE: Eur.Phys.J. C73 (2013) no.6, 2456

Diffraction in run II

- At the end of Run I the **ALICE Diffractive** detector (**AD**) was installed and commissioned, with the aim of increasing the pseudorapidity coverage and the sensitivity of ALICE to low mass diffractive systems.
- Two stations, ADA and ADC, located at z=-19.6 and z=17.0 meters respectively from the interaction point (IP).

ALICE detectors in run II

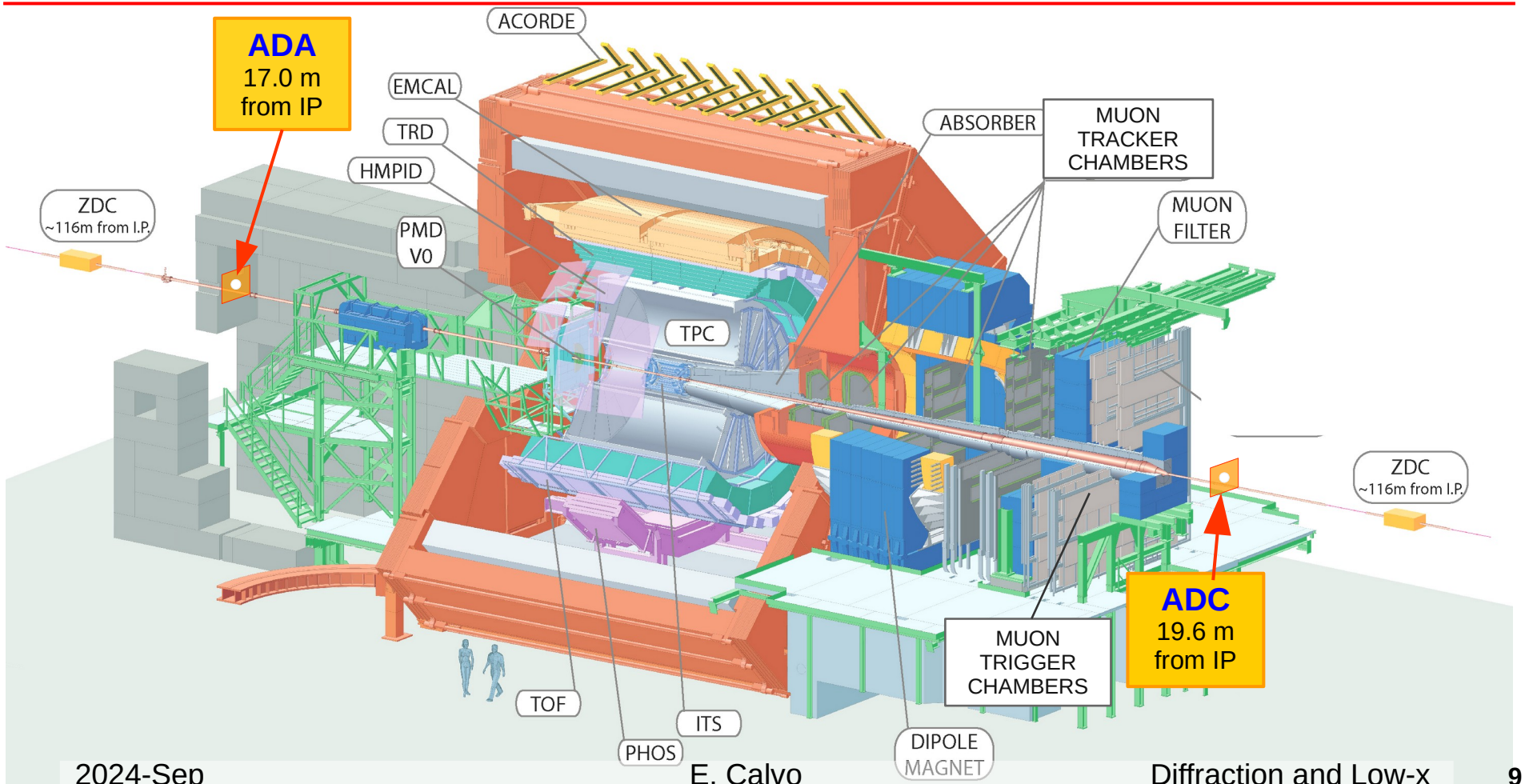

ALICE detectors in run II (A-side)

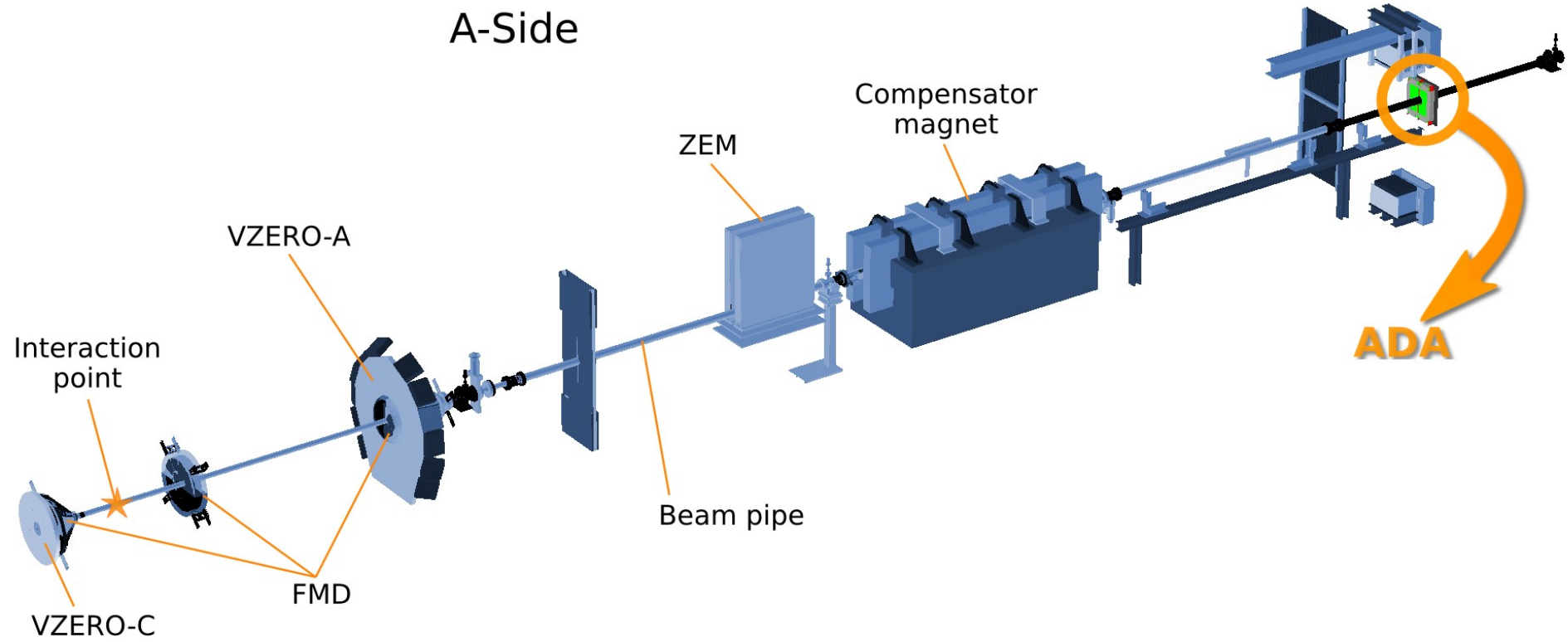

ALICE detectors in run II (C-side)

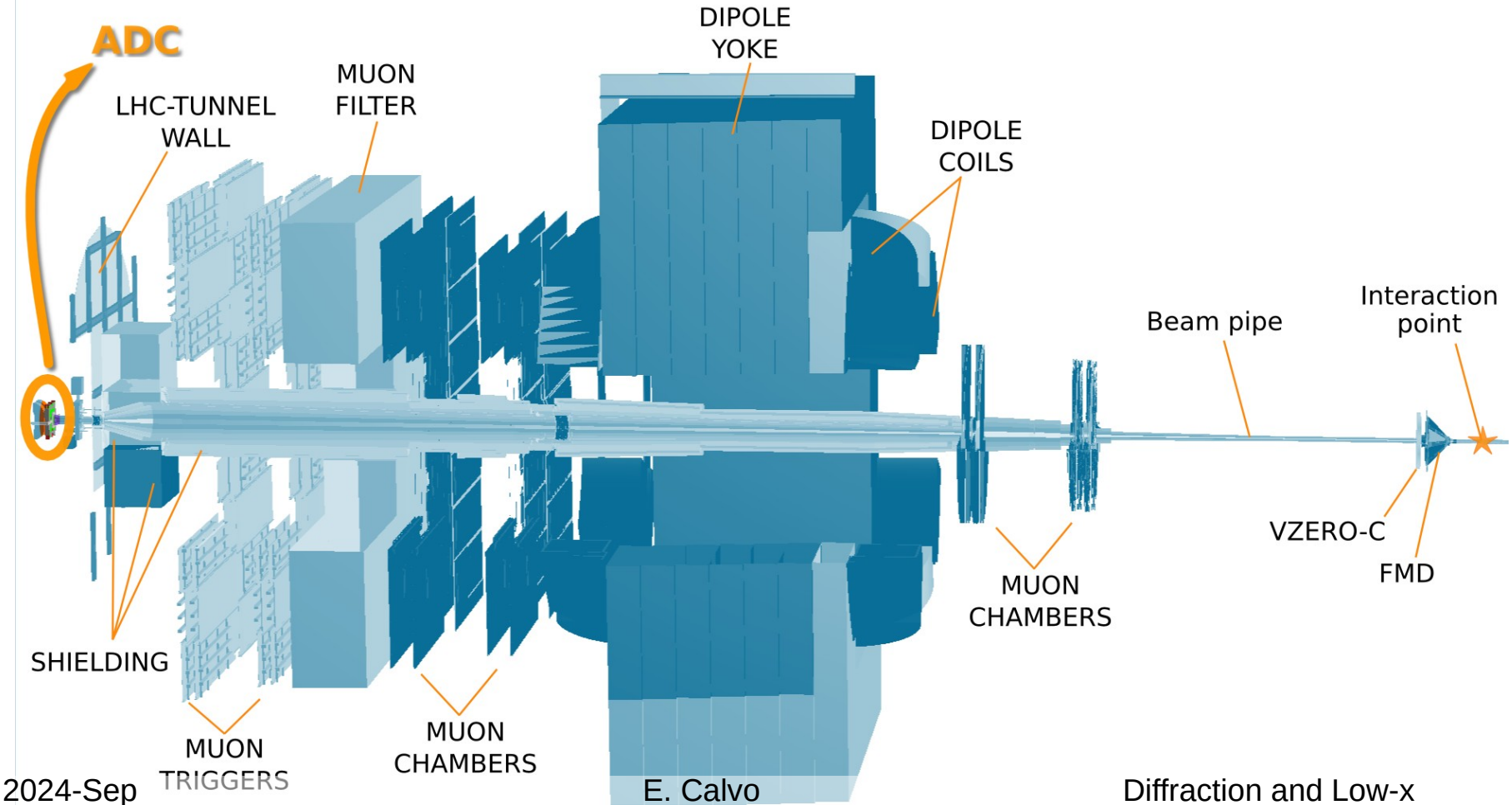

ADA and ADC extend the pseudorapidity coverage of ALICE.

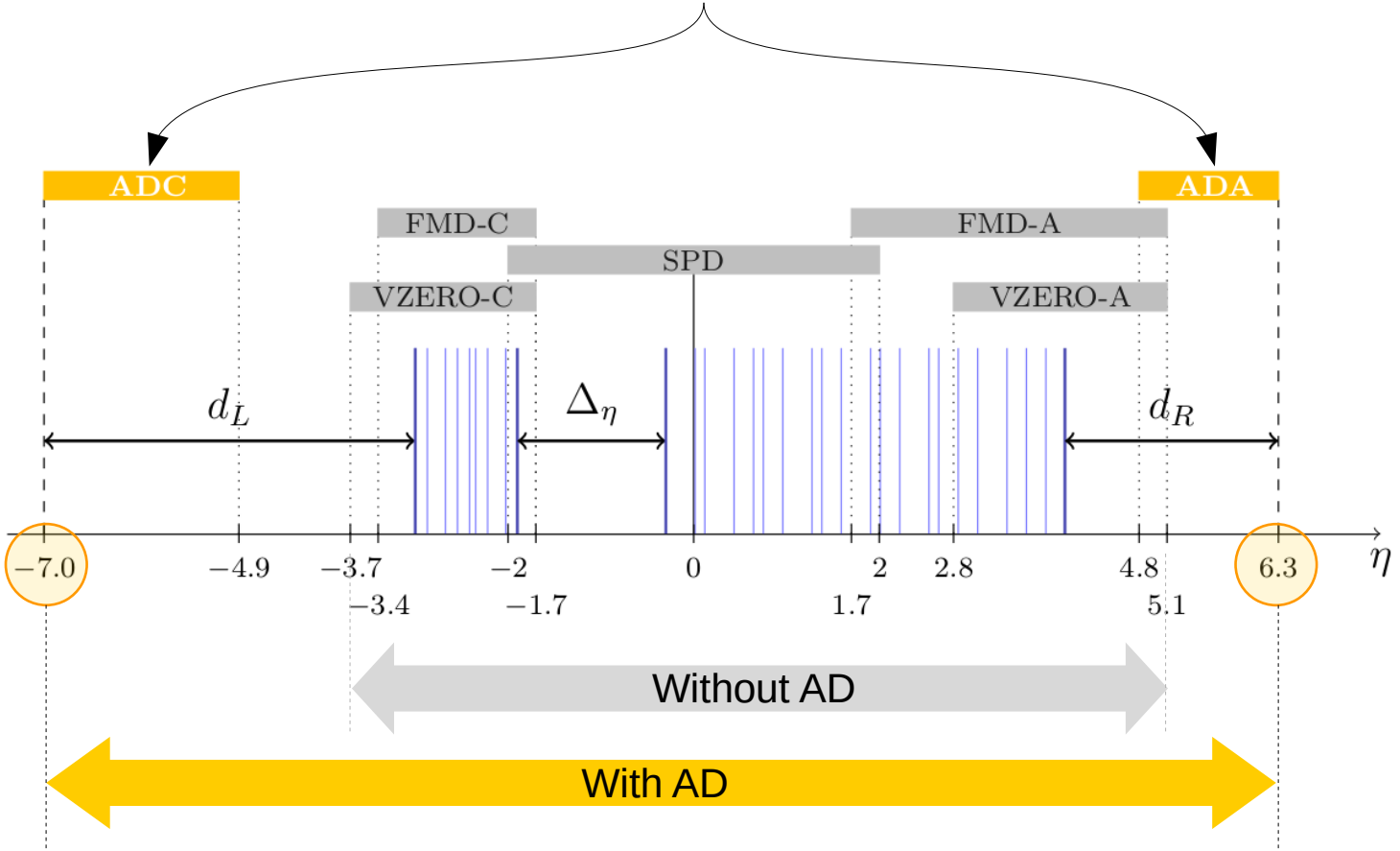

Diffractive mass and pseudorapidity

- In single diffraction, the lower the diffractive mass (M_X) the higher the odds of the event being produced.
- Moreover, there is a correlation between the M_X and the pseudorapidity of the produced particles.
  - The lower the M_X the higher the pseudorapidity.
  - This also means larger gaps at low M_X
- Hence, it is crucial to count with very forward detectors.
- ADA/ADC detectors allow ALICE to expand its pseudorapidity coverage.

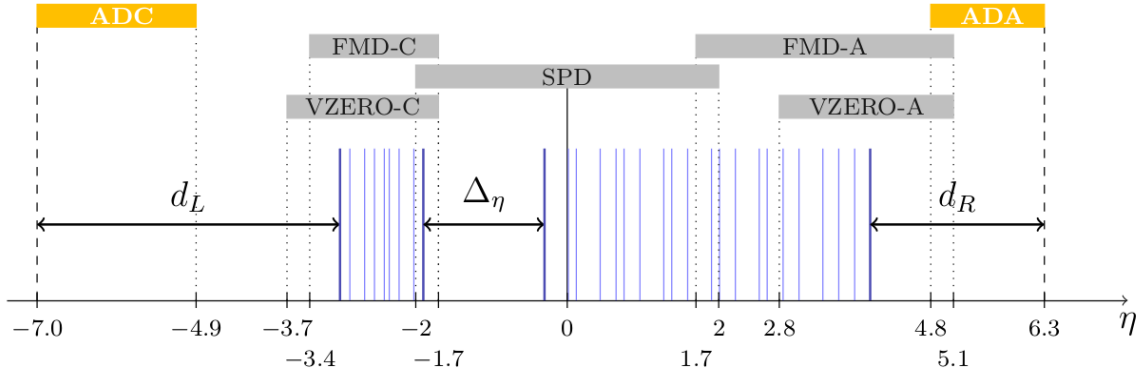

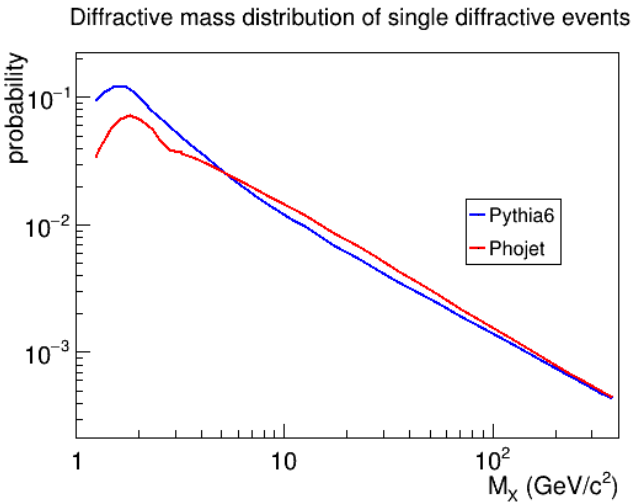

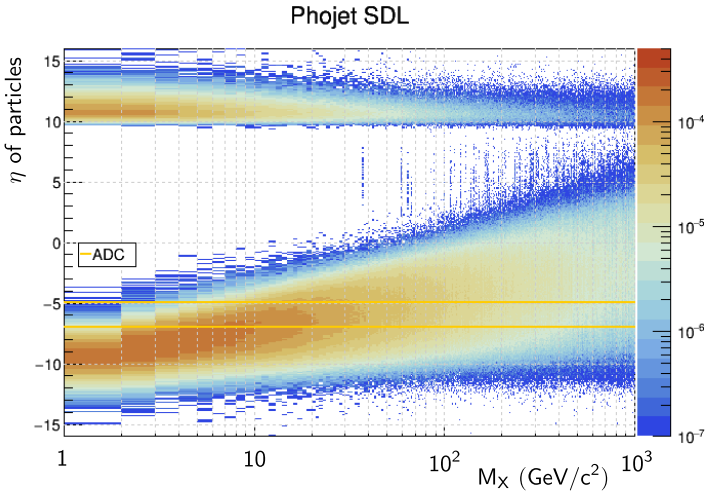

AD improves trigger efficiency for diffractive events at low diffracted masses.

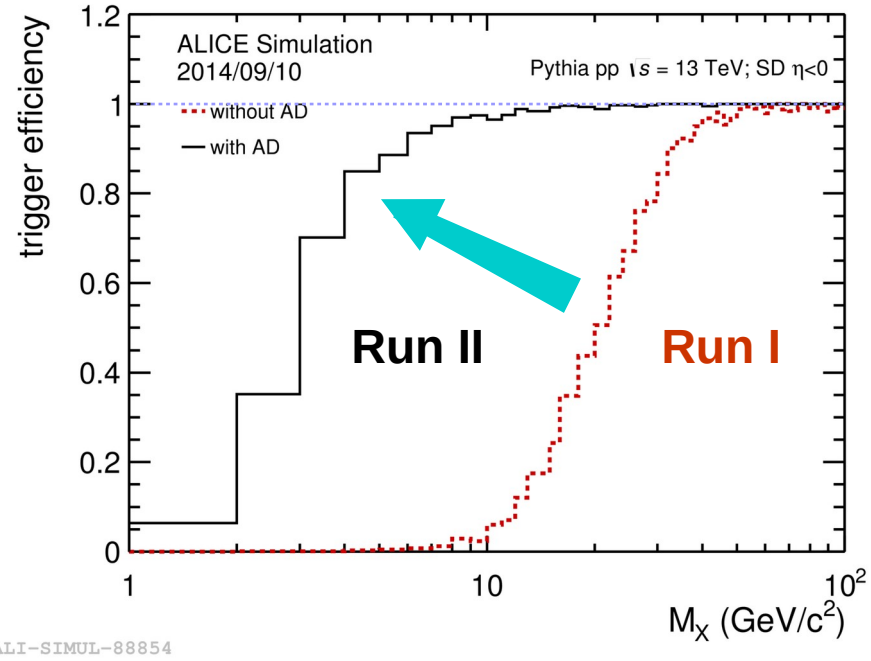

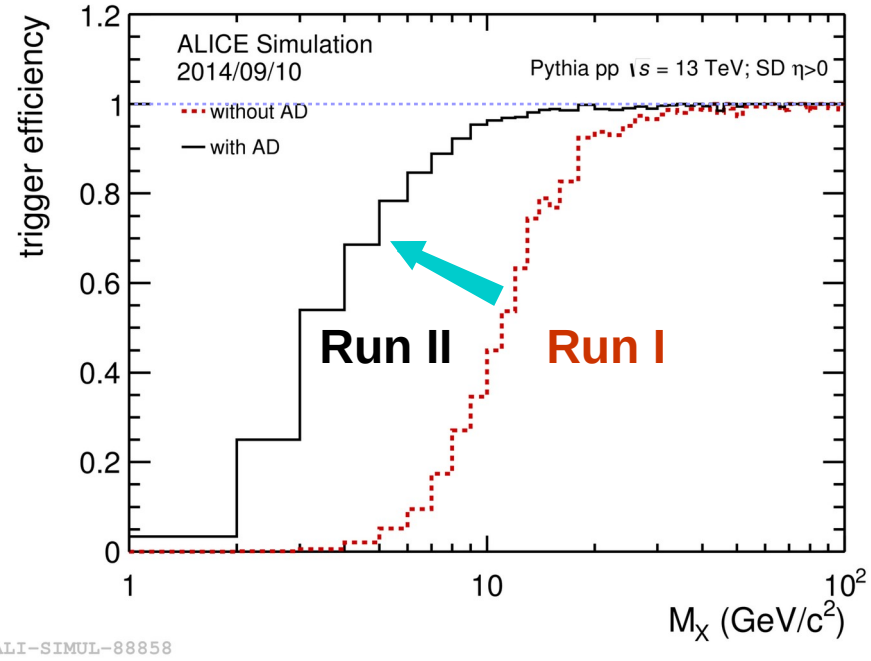

Run I :	MB_{OR} = V0C + SPD + V0A
Run II:	MB_{OR} = **ADC** + V0C + SPD + V0A + **ADA**

Event categories

There are 3 event categories:

1-arm-L → **SD-L** (left or η<0)
1-arm-R → **SD-R** (right or η>0)
2-arm → **ND** and **DD** events

DD: 2-Arm and Δη>3

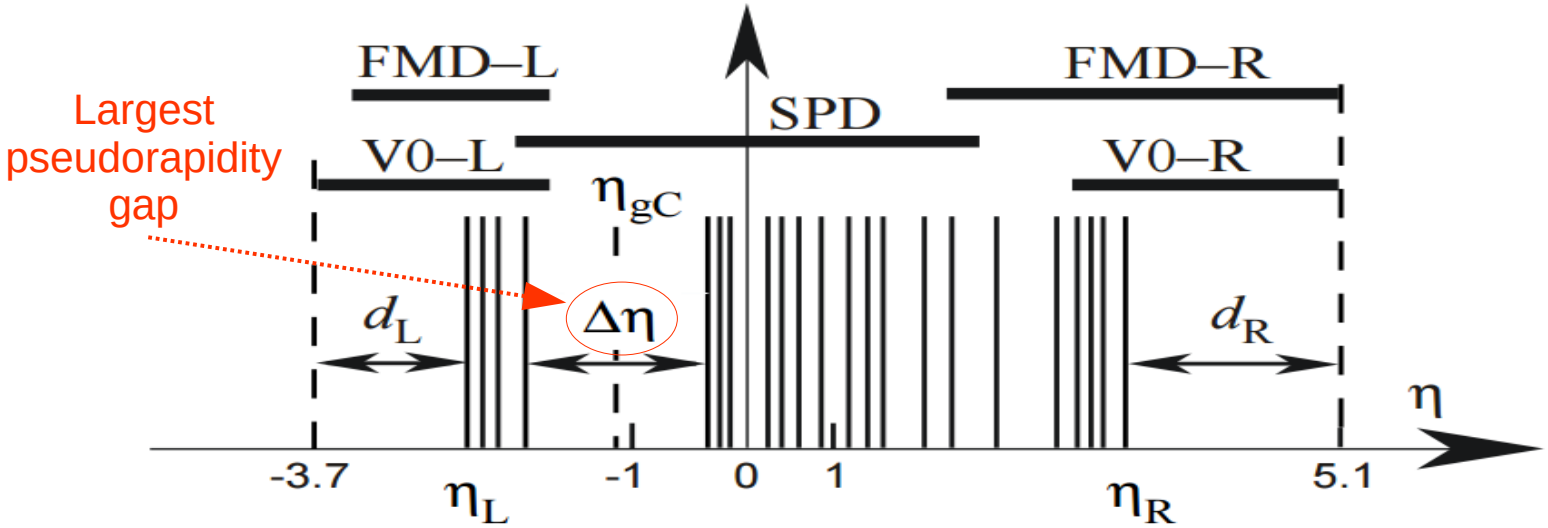

Method

$$\begin{pmatrix} \sigma_{\text{arm-L}} \\ \sigma_{\text{arm-R}} \\ \sigma_{\text{2-arm}} \end{pmatrix} = \begin{pmatrix} \epsilon^{\text{SDL}}_{\text{arm-L}} & \epsilon^{\text{SDR}}_{\text{arm-L}} & \epsilon^{\text{NSD}}_{\text{arm-L}} \\ \epsilon^{\text{SDL}}_{\text{arm-R}} & \epsilon^{\text{SDR}}_{\text{arm-R}} & \epsilon^{\text{NSD}}_{\text{arm-R}} \\ \epsilon^{\text{SDL}}_{\text{2-arm}} & \epsilon^{\text{SDR}}_{\text{2-arm}} & \epsilon^{\text{NSD}}_{\text{2-arm}} \end{pmatrix} \begin{pmatrix} \sigma_{\text{SDL}} \\ \sigma_{\text{SDR}} \\ \sigma_{\text{NSD}} \end{pmatrix}$$

observable cross sections | **detector and trigger efficiency** | **physical cross sections**

The visible cross sections of the $\sigma_{\text{arm-L}}$, $\sigma_{\text{arm-R}}$ and $\sigma_{\text{2-arm}}$ event classes are a linear combination of the physical cross sections and the trigger efficiencies: σ_{SDL}, σ_{SDR}, σ_{DD}, σ_{CD} and σ_{ND}.
The terms $\epsilon^{\text{NSD}}_{\text{arm-L}}$, $\epsilon^{\text{NSD}}_{\text{arm-R}}$ and $\epsilon^{\text{NSD}}_{\text{2-arm}}$ depend on the DD content.

$$\epsilon^{\text{NSD}}_{\text{arm-L}} = \frac{\left(f_{\text{DD}}\epsilon^{\text{DD}}_{\text{arm-L}} + f_{\text{CD}}\epsilon^{\text{CD}}_{\text{arm-L}} + f_{\text{ND}}\epsilon^{\text{ND}}_{\text{arm-L}}\right)}{f_{\text{DD}} + f_{\text{CD}} + f_{\text{ND}}}$$

$$\epsilon^{\text{NSD}}_{\text{arm-R}} = \frac{\left(f_{\text{DD}}\epsilon^{\text{DD}}_{\text{arm-R}} + f_{\text{CD}}\epsilon^{\text{CD}}_{\text{arm-R}} + f_{\text{ND}}\epsilon^{\text{ND}}_{\text{arm-R}}\right)}{f_{\text{DD}} + f_{\text{CD}} + f_{\text{ND}}}$$

$$\epsilon^{\text{NSD}}_{\text{2-arm}} = \frac{\left(f_{\text{DD}}\epsilon^{\text{DD}}_{\text{2-arm}} + f_{\text{CD}}\epsilon^{\text{CD}}_{\text{2-arm}} + f_{\text{ND}}\epsilon^{\text{ND}}_{\text{2-arm}}\right)}{f_{\text{DD}} + f_{\text{CD}} + f_{\text{ND}}}$$

Simulation of single diffraction

- Before we proceed, we need to improve the description of single diffraction in the MC generators. The main uncertainty in the simulation of diffraction is the shape of the single diffractive mass distribution.
- In similar way as the 2012 ALICE paper[(a)], the Kaidalov-Poghosyan (KP) model is used. Weights are applied to the generated SD events.
- Two linear variations of this model are also used in order to account for theoretical uncertainty.
- If M_X>200 GeV/c^2 → event is relabeled as non-diffractive.

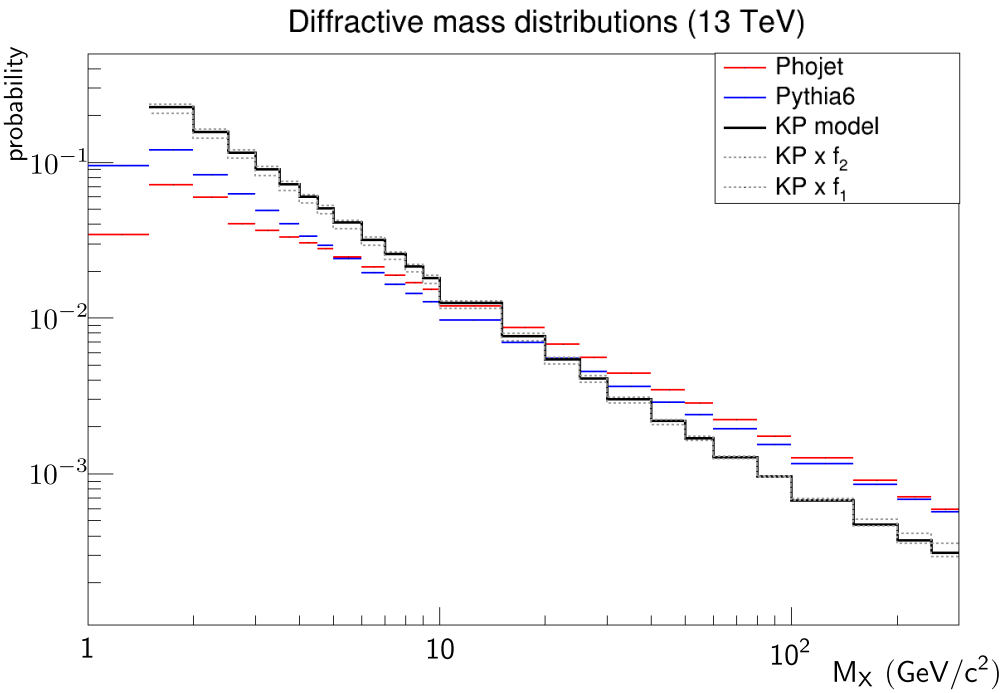

(a) Eur.Phys.J. C73 (2013) no.6, 2456

Extracting the DD content (without AD)

Here, events have been selected by the 2-arm condition (mostly non-diffractive and double-diffractive).

The distribution of the largest gap per event is plotted for data and MC.

The double-diffractive content of Pythia 6 (Phojet) is tuned in order to better follow the data distribution from above (below).

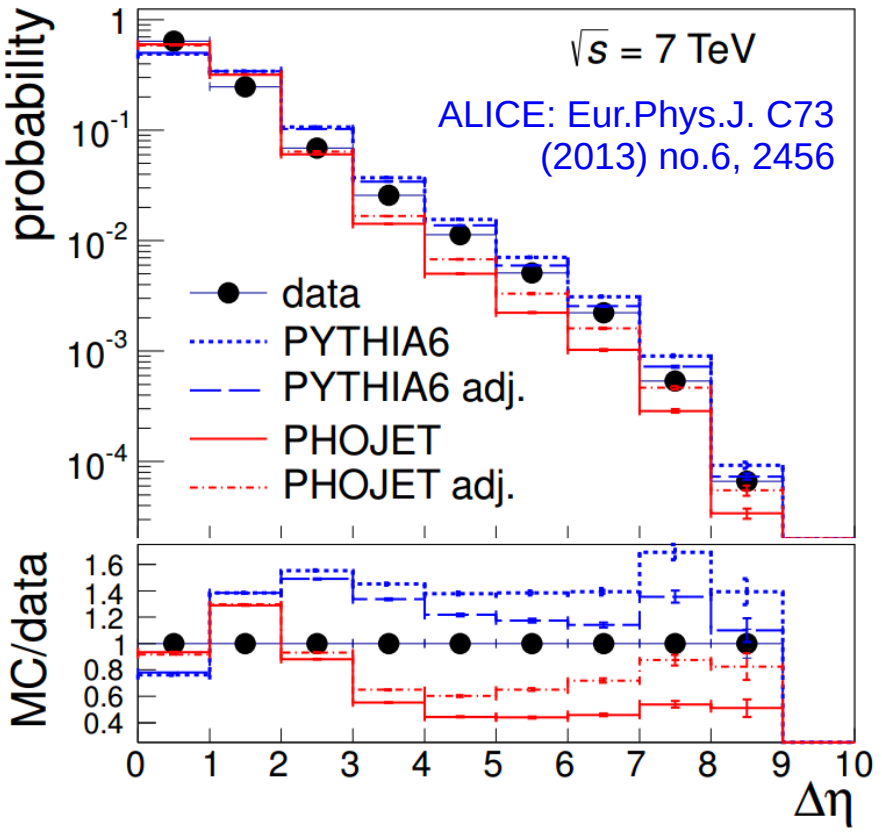

Extracting relative cross sections

Extract $\sigma_{\mathrm{DD}}/\sigma_{\mathrm{INEL}}$: Using largest gap in 2-arm events, tune the DD fraction in MC until it brackets the data. If this is the first iteration then use default $\sigma_{\mathrm{SD}}/\sigma_{\mathrm{INEL}}$ values for MC.

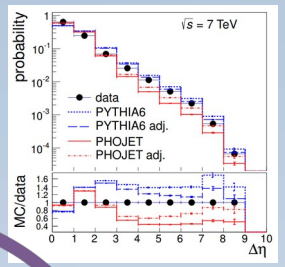

ALICE: Eur.Phys.J. C73 (2013) no.6, 2456

1

Use this $\sigma_{\mathrm{DD}}/\sigma_{\mathrm{INEL}}$ to update 1,2-arm efficiencies to NSD processes (i.e., $\epsilon^{\mathrm{NSD}}_{\text{arm-L}}$, $\epsilon^{\mathrm{NSD}}_{\text{arm-R}}$ and $\epsilon^{\mathrm{NSD}}_{\text{2-arm}}$)

2

With $\sigma_{\mathrm{SD}}/\sigma_{\mathrm{INEL}}$, $\sigma_{\mathrm{DD}}/\sigma_{\mathrm{INEL}}$ and new efficiencies iterate until you reach desired level of precision

Calculate $\sigma_{\mathrm{SD}}/\sigma_{\mathrm{INEL}}$, with the $\sigma_{\mathrm{DD}}/\sigma_{\mathrm{INEL}}$ and the updated efficiencies obtained in previous steps. This implies solving the linear system shown right

$$\begin{pmatrix} \sigma_{\text{arm-L}} \\ \sigma_{\text{arm-R}} \\ \sigma_{\text{2-arm}} \end{pmatrix} = \begin{pmatrix} \epsilon^{\mathrm{SDL}}_{\text{arm-L}} & \epsilon^{\mathrm{SDR}}_{\text{arm-L}} & \epsilon^{\mathrm{NSD}}_{\text{arm-L}} \\ \epsilon^{\mathrm{SDL}}_{\text{arm-R}} & \epsilon^{\mathrm{SDR}}_{\text{arm-R}} & \epsilon^{\mathrm{NSD}}_{\text{arm-R}} \\ \epsilon^{\mathrm{SDL}}_{\text{2-arm}} & \epsilon^{\mathrm{SDR}}_{\text{2-arm}} & \epsilon^{\mathrm{NSD}}_{\text{2-arm}} \end{pmatrix} \begin{pmatrix} \sigma_{\mathrm{SDL}} \\ \sigma_{\mathrm{SDR}} \\ \sigma_{\mathrm{NSD}} \end{pmatrix}$$

- We iterate until we reach final values.
- At this stage we have extracted the relative content of DD and SD in MC.
- The main uncertainty in DD comes from the difference between Pythia6 and Phojet. In SD, the uncertainty comes from the variations of KP model used to account for the theoretical uncertainty in the shape of M_X distribution.
- Work to get final values is ongoing.

Summary and outlook

- Inelastic and diffractive cross sections were measured by ALICE in run I in p-p collisions at 7 TeV, with results consistent with other experiments.
- At 13 TeV, one of the main uncertainties is the low efficiency of detecting single diffractive events at low diffracted masses.
- Forward detectors like ADA and ADC, increase pseudorapidity coverage and reduce uncertainty in measurement of relative cross sections. Study of inelastic and diffractive cross sections at 13 TeV is progressing (run II).
- During the ongoing run III ALICE has already surpassed the amount of p-p data collected during run II. The AD detectors, now rebranded as FDD and continue to take data as part of the FIT detector, which poses interesting possibilities for future diffractive studies.

Back-up slides

ADC Detector

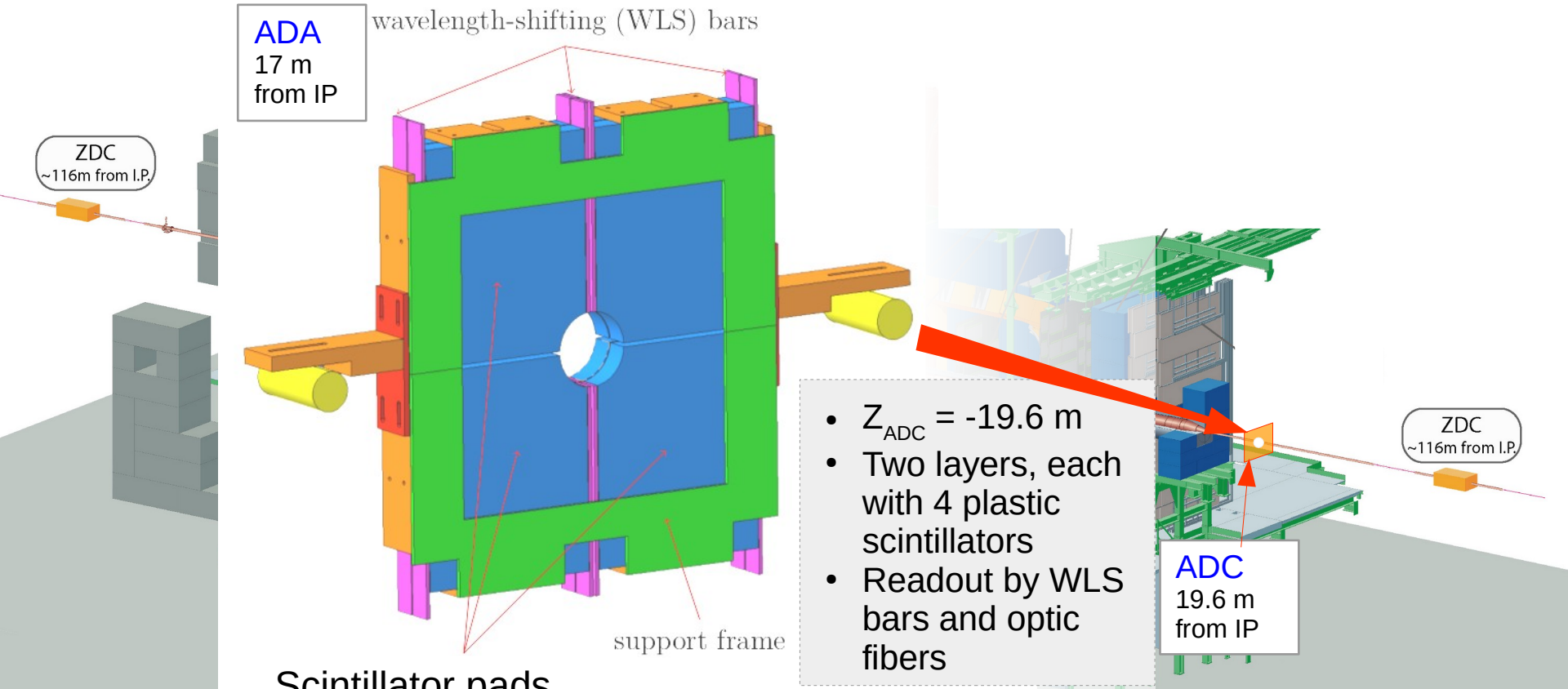

- Z_{ADC} = -19.6 m
- Two layers, each with 4 plastic scintillators
- Readout by WLS bars and optic fibers

Scintillator pads

ADA Detector

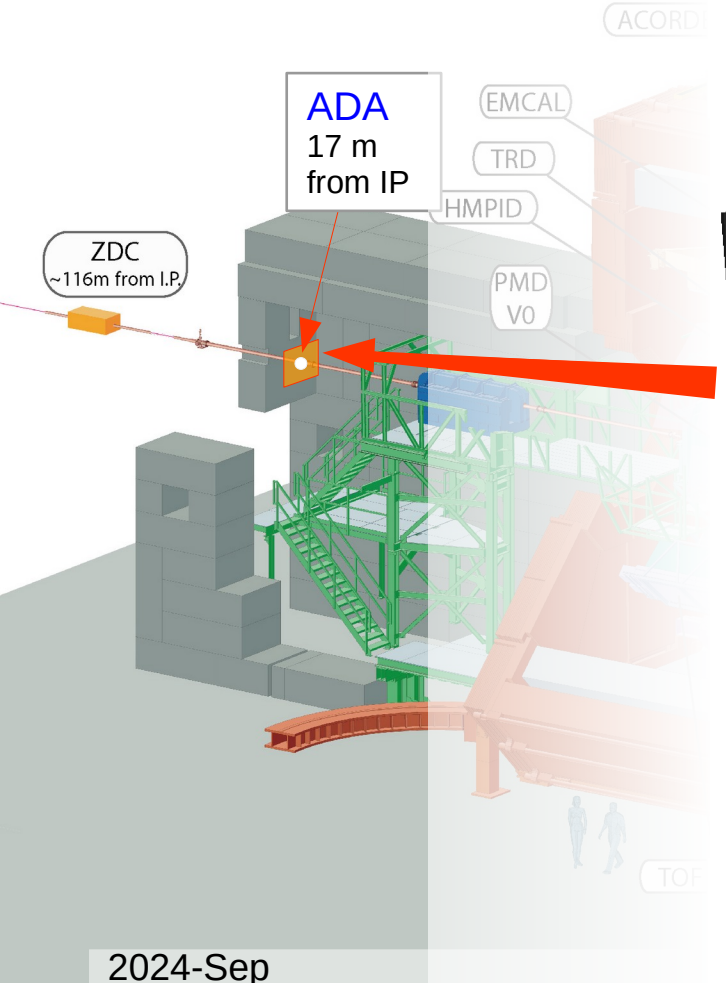

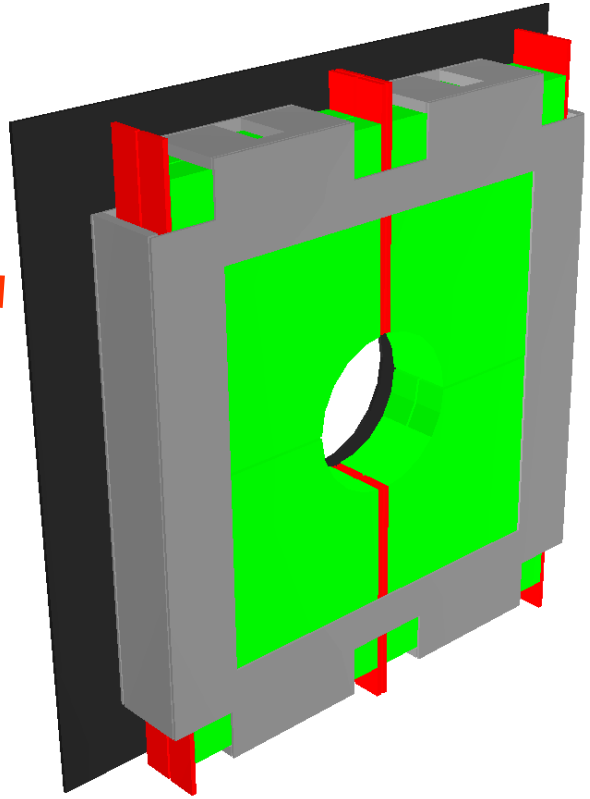

- Z_{ADA} = +17.0 m
- Two layers, each with 4 plastic scintillators
- Readout by WLS bars and optic fibers